

# Heat Transfer and Pressure Drop Characteristics in a packed bed Solar Air Heater

L. VARSHNEY, RAMESHWAR KUMAR SINGH

Department of Mechanical Engineering

College of Technology

G. B. Pant University of Ag. & Technology

Pantnagar-263145,

INDIA

lvarshney20@gmail.com

**Abstract** - In the present work an experimental setup has been designed and fabricated for the experimental investigations on a packed bed solar air heater under simulated conditions. Wire mesh screen matrices with different geometrical parameters have been used as packing element in the flow duct. Data pertaining to heat transfer and friction factor characteristics were collected for air flow rate ranging from 0.0101 to 0.0250 kg/s.m<sup>2</sup> for five sets of matrices with varying geometrical parameters. The thermal efficiency of packed bed solar air heater was compared with that of a conventional solar heater. Enhancement in the thermal efficiency, of the order of 41.15 to 82.40% was obtained as compared to conventional smooth solar collector under similar operating conditions investigated in the present work.

The effect of geometrical parameters (wire diameter, pitch, porosity and number of layers) of matrices on the heat transfer coefficient and pressure drop, which affect the thermal efficiency of the collector, has been discussed in detail.

**Key words**- Solar collector, packed bed, geometrical parameters, wire mesh, air heater, heat transfer

## 1. Introduction

Solar air heaters are the cheapest and extensively used solar energy collection devices employed to deliver heated air at low to moderate temperatures for space heating, drying agricultural products such as fruits, seeds and vegetables, and some industrial applications. Such air heaters have low thermal efficiency because of low convective heat transfer coefficient between the absorber plate and air leading to higher temperature of the absorber plate, which results in higher heat losses to the surroundings. Several methods including the use of packing of porous materials like wire screens, Cross rod matrices and slit and aluminium-foil matrices in the duct of solar air heater have been proposed for the enhancement of thermal performance of the solar air heater (Coppage and London, 1965; Tong and London, 1957; Kays and London, 1964; Chiou et al., 1965; Hamid and Beckman, 1971; Hasatani et al., 1985; Choudhary and Garg, 1993; Ozturk and Demirel, 2004; Thakur et al. 2003; Mittal and Varshney, 2006; Varshney and Saini 1998).

It has been found that packing of wire-mesh screen or other suitable packing element is an easy and effective way for improving the performance of packed bed solar air heaters (Prasad et al., 2009;

Dhiman et al., 2012). Wire screens are also suited as packing element as their geometries are completely known and wider range of geometrical parameters can be generated using wire screens of various diameter and pitch.

The thermo-hydraulic investigations of a solar air heater packed with wire screen matrices for different geometrical parameters were done by Mittal and Varshney (2006). A design criterion was suggested to select a matrix for packing the flow channel which would result in best thermal performance with minimum pumping power penalty.

Thakur et al. (2003) have experimentally investigated the heat transfer and fluid flow characteristics of solar air heater packed with mesh screen matrices for a range of porosity 0.667-0.880. These investigations reveal that there is substantial rise in volumetric heat transfer coefficient with a decrease in porosity. This investigation appears to be at variance with other studies performed (Varshney and Saini, 1998; Mittal and Varshney 2006). These investigations were performed under actual outdoor conditions, where the heat flux is not completely stable. Hence, higher porosity system would be a better choice when one looks for the

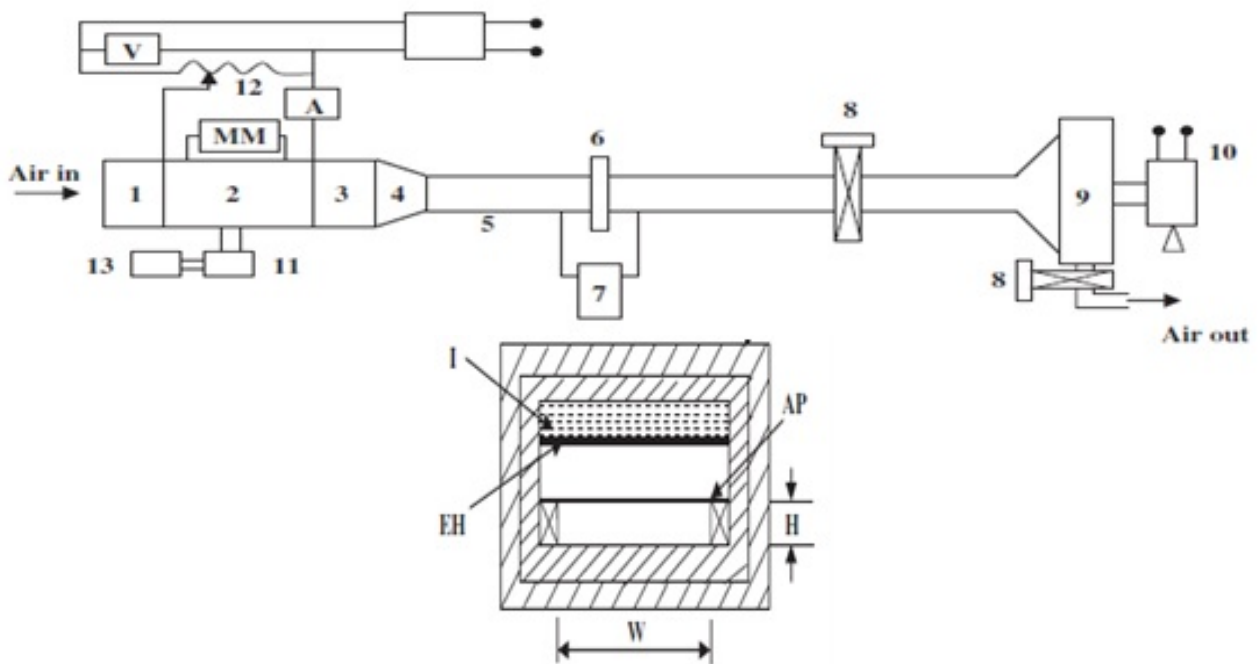
enhancement of the thermal performance of a packed bed solar air heater having wire mesh screen matrices.

Therefore, it was decided to investigate the effect of porosity on heat transfer and fluid flow for a higher range of porosity under simulated conditions. This paper presents the details of an investigation of the heat and fluid flow characteristics of packed bed solar air heater for a relatively high porosity range from 0.932 to 0.969. Tests were conducted under simulated conditions with constant heat flux for a packed bed solar air heater and a conventional solar air heater in order to compare their thermal performance.

## 2. Experimental Set-up

Fig.1 shows the schematic of an experimental set-up and Fig.2 shows the Sectional view of rectangular solar air duct that has been designed and fabricated to collect data with respect to heat transfer and

93-77 (1977). The set-up consists of an entry section, a test section and an exit section. The size friction characteristics of a packed bed solar air heater in accordance with ASHRAE STANDARD of the entire duct is 2150 mm x 320 mm x 25 mm, out of which 1000mm is the length of test section. The length of entry and exit sections are 650 and 500 mm, respectively. In the smooth duct, the bottom is made of 35 mm thick soft wood. The side walls of the duct are made of 25 mm thick soft wood. Inside the duct, batons of 20 mm width are fixed adjacent to the side walls providing a height of 25 mm. A 2 mm aluminium sheet (absorber plate) is fixed on these batons. Entry section is provided towards the inlet side of the test duct to enable the flow to stabilize and become uniform before it enters the test section. The entry section is made up of soft wood having the same cross sectional area as that of the test section. The length of the entry section is 650 mm in accordance with the design considerations.



- 1. Entry Section
- 3. Exit Section
- 5. G. I. Pipe
- 7. U-tube Manometer
- 9. Centrifugal Blower
- 11. Selector Switch
- 13. Temperature Indicator

- 2. Test Sect
- 4. Mixing Plenum
- 6. Orifice Plate
- 8. Control Valves
- 10. Electric Motor
- 12. Voltage Variac
- MM- Micro Manometer

- I -Insulation
- AP- Absorber Plate
- H- Duct Height
- W-Duct Width
- E-Electric Heater
- A-Ammeter
- V-Voltmeter

Fig. 1. Schematic Diagram of Experimental Setup

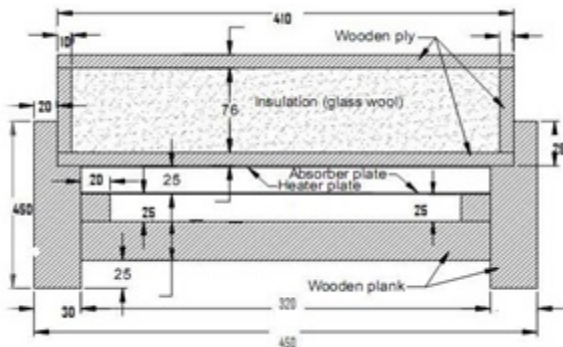


Fig.2 Sectional view of rectangular solar air heater duct

Wooden exit section is provided towards the outlet of the test duct which is followed by mixing device (baffles) for mixing the air. This is necessary because temperature gradient exist along the depth in the stream of the air coming out of the test ducts. The length of the exit section is 500 mm and the cross section matches with that of the test duct. Three equi-spaced baffles are provided spread in 100 mm length beyond the exit section which is made up of aluminium sheet for the purpose of mixing hot air coming out of the duct. One baffle is fixed on the bottom side and the remaining two on the upper side. Length of the baffles is equal to the width of the mixing section. Mixing section is connected to the M.S. pipe fittings through transition piece and flexible pipes. A centrifugal air blower with single phase, 3.0 h.p. (2.2 kW) motor is provided with its suction end connected to the M.S. pipes to force the air through the test ducts. To regulate and maintain a particular flow rate through the test duct, an gate valve is provided with pipe line. For the measurement of rate of air flow through the test ducts, orifice plate has been used. The orifice plate is fixed between two flanges fixed with straight M.S. pipe having 80 mm inner diameter. The length of the M.S. pipe upstream, of the orifice meter was 1000 mm and towards the downstream of the orifice plate was 500 mm. Flange taps are provided at a distance of 80 and 40 mm on each side of the orifice plate. For temperature measurements 28 SWG pre calibrated copper-constantan thermocouples are used. After the fabrication of the set-up data have been collected on the packed bed solar air heater. Similar data have been also been collected on the conventional solar air heater for the purpose of comparison in enhancement of thermal efficiencies.

### 3. Validation Of Experimental Set-Up

Before collecting data the system was validated by collecting data for the system with conventional

(smooth) duct. Nusselt Number and friction factor were determined for smooth duct for different mass flow rates. Values of these parameters obtained experimentally were compared with predicted values of Nusselt Number using correlation given by Gneilinski and friction factor using Dittus and Boelter correlation (Bhatti and Shah, 1987).

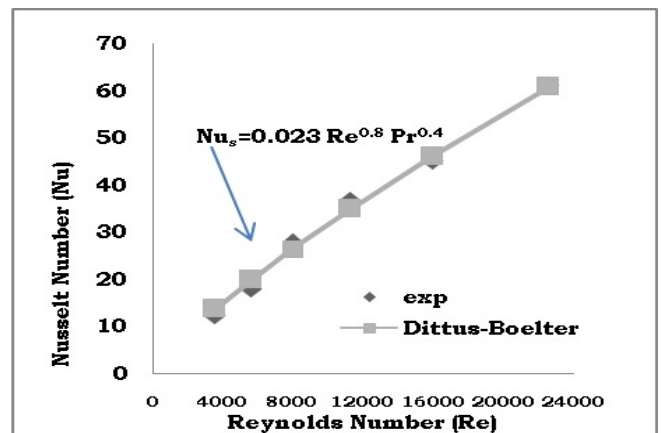


Fig.3 Comparison of experimental and predicted values of Nusselt number for smooth duct

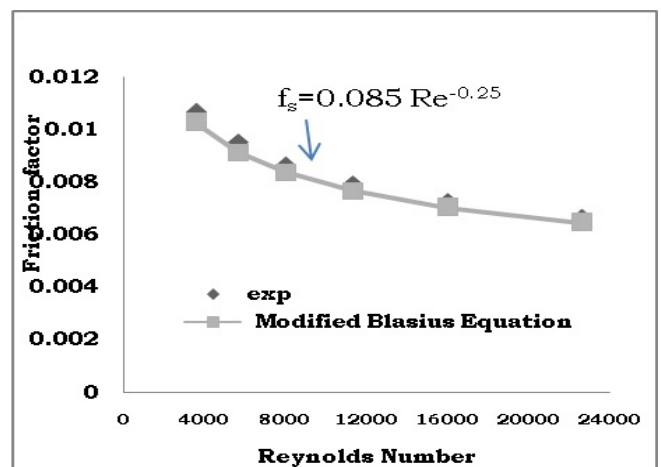


Fig.4 Comparison of experimental and predicted Values of friction factor for smooth duct

Figs. 3 and 4 show a comparison between experimental and predicted values of Nusselt Number having a maximum deviation of 6.92% while the friction factor has a maximum deviation of 3.11% from the predicted values. This ensures the reliability of experimental set up for further investigation for performance studies of solar heater having wire screen matrixes as listed in Table 1.

Table 1. Geometrical parameter of wire screen matrices of the packed bed solar air heater

Packing	Wire dia of screen (mm)	Pitch (mm)	No. of layers	Bed depth	Effective porosity	Heat transfer area	Hydraulic radius (m)×10 <sup>3</sup>
M1	0.36	2.69	10	25.0	0.969	2.755	2.81
M2	0.36	2.69	8	25.0	0.975	2.222	3.51
M3	0.585	3.17	10	25.0	0.932	3.719	2.01
M4	0.585	3.17	8	25.0	0.945	3.008	2.51
M5	0.585	3.17	6	25.0	0.959	2.242	3.42

#### 4. Analysis Of Experimental Data

For a packed bed, mass flow rate ( $G_0$ ) is given by:

$$G_0 = \frac{m}{A_f P} \quad (1)$$

Where,  $m$  is the mass flow rate of the air.

Packed bed Reynolds number ( $Re_p$ ) is defined as:

$$Re_p = \frac{4r_h G_0}{\mu} \quad (2)$$

The heat transfer rate ( $Q_u$ ) to the air can be determined as:

$$Q_u = m C_p (t_o - t_i) \quad (3)$$

Where,  $t_o$  and  $t_i$  are the outlet and inlet temperature of the air respectively.

The average convective heat transfer coefficient ( $h_c$ ) between wire screen matrices and the flowing air is given by

$$h_c = \frac{Q_u}{A(\bar{t}_{me} - \bar{t}_f)} \quad (4)$$

Where,  $\bar{t}_{me}$  is the average matrix temperature based on the average of the temperature measurement made along the length and depth of the packed bed and  $\bar{t}_f$  is the average air temperature.

Using the average value of heat transfer coefficient ( $h_c$ ) given by equation (4), the Stanton number, and colburn  $J_h$  factor can be evaluated using the following relations:

$$St = \frac{h_c}{(G_a C_p)} \quad (5)$$

$$J_h = St \cdot Pr^{2/3} \quad (6)$$

Using the pressure drop data, the friction factor ( $f_p$ ) can be evaluated using the relation:

$$f_p = \frac{\rho u \Delta P L}{\rho u^3 / 2g_m} \quad (7)$$

where,  $\Delta P$  is the pressure drop in packed duct and  $u$ , the air velocity in the packed duct is calculated as follows:

$$u = \frac{G_0}{\rho}$$

The thermal efficiency of the solar air heater can be obtained from temperature rise in the collector and is given by

$$\eta = \frac{G C_p \Delta t}{I} \quad (8)$$

where  $G = m/A_c$ ,  $A_c$  is the collector area and  $I$  is the insolation.

The experimental data were used to determine the values of various parameter as given above. The properties of air, namely density, viscosity, specific heat and Prandtl number used in the calculation, were evaluated at the arithmetic mean of the inlet and outlet temperature of air.

### 5. Results And Discussion

The raw data collected have been processed to determined the value of thermal efficiency, heat transfer coefficient and friction factor. The result are discussed below.

#### 5.1 Effect of Reynolds number on Nusselt number (Nu)

Figure 5 shows the variation of Reynolds number on Nusselt numbers for different wire screen matrices. Nusselt number increases with increase in Reynolds number for all the matrices. This is obvious as with the increase in the Reynolds number, the turbulence increases which increase the heat transfer coefficient and accordingly the Nusselt Number increases. It is also observed that the heat transfer coefficient enhancement is maximum for matrix M5 and minimum for matrix M3. The values of Nusselt number increases from 6.08 to 51.53 for increase in Reynolds number from 625.3 to 2619.9.

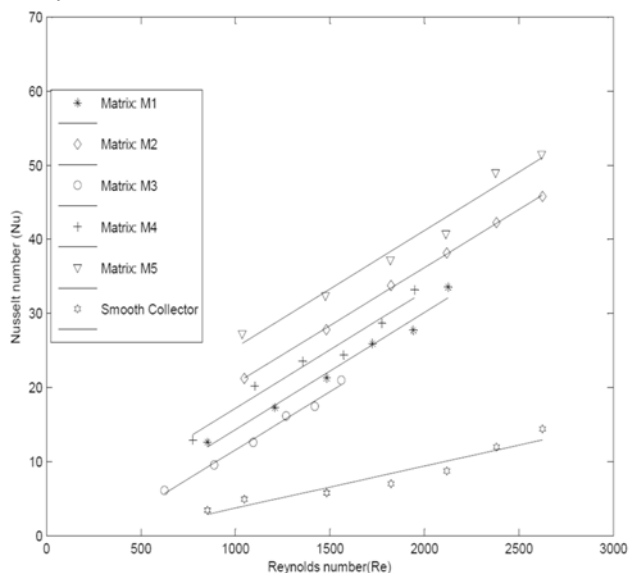


Fig.5. Effect of Reynolds number on Nu for different matrix

#### 5.2. Effect of Reynolds number on Friction factor

Figure 6 shows the variation of friction factor with Reynolds number for different wire screen matrices. The friction factor is minimum for matrix M5 and maximum friction factor occurs for matrix M3 for the entire range of Reynolds number investigated. The friction factor for matrix M1, M2 and M4 is lies between the matrix M3 and M5, however the values of friction factor are always higher as compared to smooth collector. It is also observed that the value of friction factor reduces with the increase in Reynolds number. Friction factor is found to be

minimum for matrix M5 and maximum for matrix M3 out of the matrices investigated.

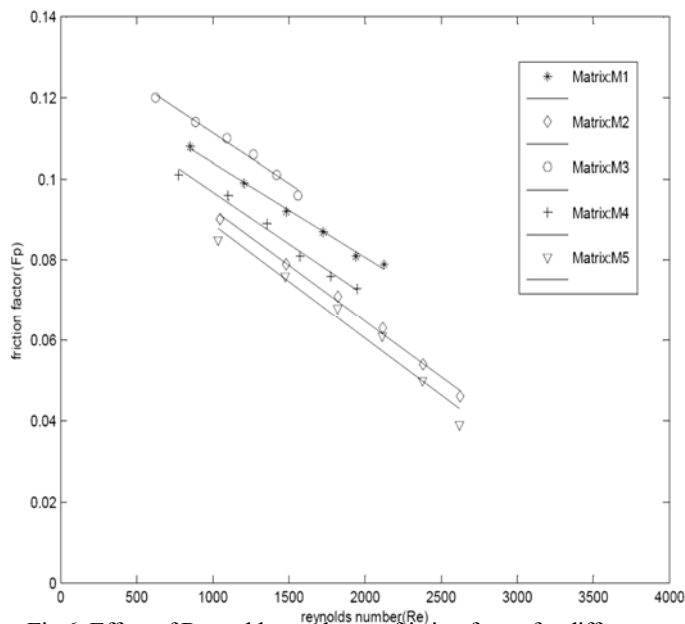


Fig.6. Effect of Reynolds number on friction factor for different matrix

#### 5.3. Thermal performance of solar air heater

Performance plots are drawn in Fig. 7 and 8 for matrix M3 and M5 respectively following the procedure proposed by Reddy and Gupta (1980), where efficiency ( $\eta$ ) is plotted against temperature rise parameter ( $(t_o - t_i)/I$ ) each line in these plots has been drawn from first order least square fit of data points for a given set of bed parameters. Corresponding efficiency plots for data smooth collectors have also been shown in these figures.

From performance plots, it is observed that the efficiency of wire screen matrix packed air heater as well as smooth air heater increase with increase in mass flow rate and decrease with increase in temperature rise parameter ( $(t_o - t_i)/I$ ). This is an expected behavior in view of the fact for a given incident solar radiation flux ( $I$ ) and inlet temperature ( $t_i$ ) when the flow rate of air through collector decrease the value of outlet temperature ( $t_o$ ) increases. In other words when the flow rate of air increase the value of  $(t_o - t_i)$  should decrease. Performance plots also indicate a substantial enhancement in thermal efficiency of packed bed collector over smooth collector for similar operating conditions.

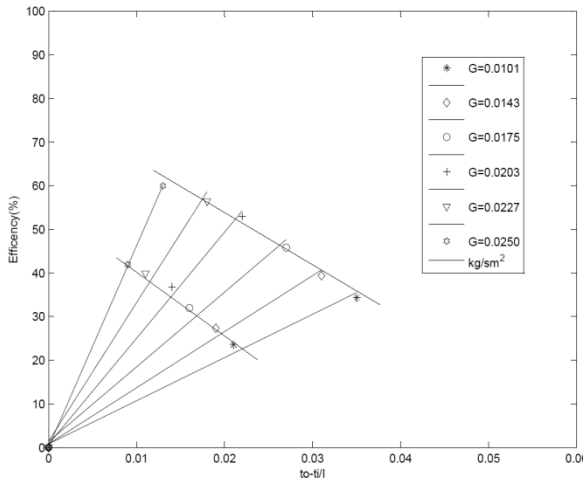


Fig. 7. Performance of packed bed air heater with matrix M3 and corresponding smooth air heater

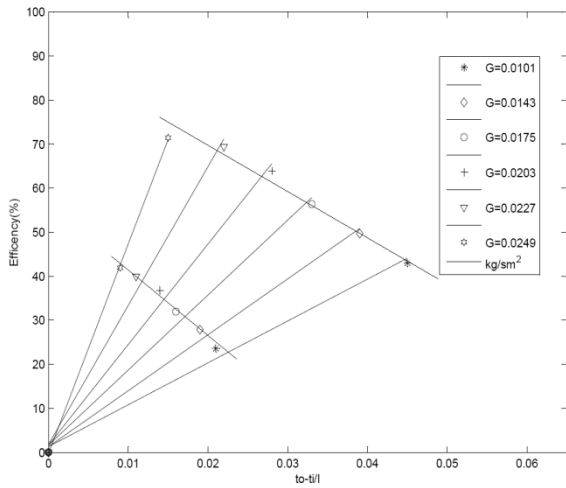


Fig. 8. Performance of packed bed air heater with matrix M5 and corresponding smooth air heater

Fig. 9 has been drawn to show the comparison of performance with different matrixes used for investigation.

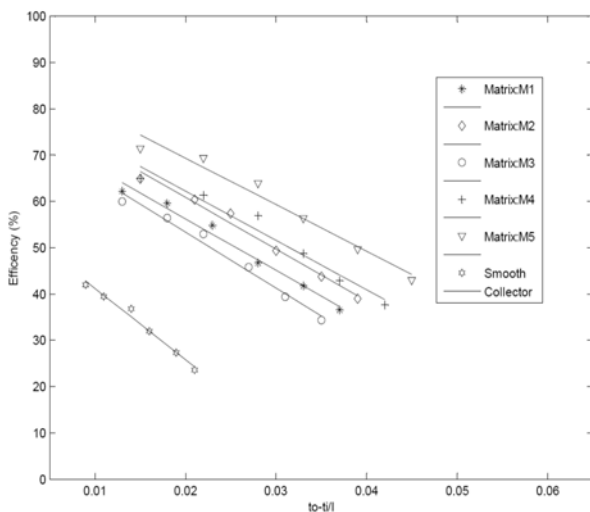


Fig. 9. Comparison of performance with different matrix and smooth air heater

Table 2 has been prepared to show the numerical values of efficiencies for packed bed air heater for different mass flow rates. Corresponding values of efficiency of air heater with wire screen matrix over smooth collector have been listed. These values correspond to extreme values of mass flow rate i.e. 0.0101 kg/s/m<sup>2</sup> to 0.0250 kg/s/m<sup>2</sup> with five set of matrices as a packing element.

For the purpose of comparison of performance of all five set of matrix, Fig. 12 has been prepared. The variation in performance seem due to varying geometrical and operating parameter. These effect can be analyzed based on the following discussion.

Table 2. Enhancement in collector efficiency

Matrix designation	G (kg/sm <sup>2</sup> )	$\eta_s$	$\eta$	Enhancement (%)
M1	0.0101	23.58	36.57	55.08
	0.0249	41.94	63.21	50.71
M2	0.0101	23.58	38.98	65.30
	0.0249	41.94	67.89	61.87
M3	0.0101	23.58	34.29	45.41
	0.0248	41.89	59.94	41.15
M4	0.0101	23.58	37.57	59.32
	0.0250	41.92	65.02	55.10
M5	0.0101	23.58	43.01	82.40
	0.0250	41.92	71.39	70.03

### 5.3.1 Effect of mass flow rate

Effect of mass flow rate on temperature rise parameter for matrix packed solar air heater has been presented in Fig. 10 it is observed from the plot that there is a decrease in temperature rise parameter for increasing mass flow rate for all the matrix as well as smooth collector. The curves for all the matrices tend to converge at high mass flow rate and difference in their relative values decrease and become only marginal. Thermal efficiency corresponding to mass flow rate have been plotted in Fig. 11 These values for all the matrices and smooth collector increase with increase in mass flow rate. At lower mass flow the rate of increase in efficiency is higher, the rate decreasing with increase with mass flow rate. This behavior as seen in Fig. 10 and 11 can be attributed to the fact that as mass flow rate decreases, the collector operate at higher temperature which contributes to higher losses. Also the convective heat transfer coefficient

increases as the air mass flow rate decreases. This causes the efficiency to increase with increasing mass flow rate. The plot also indicates that the efficiency of packed bed air heater is significantly higher compared to smooth collector. It is worthwhile to note that although increasing the mass flow rate itself increases the efficiency and the effect is quite substantial but just increasing the mass flow rate cannot be used as a method of enhancement of efficiency because it is accompanied by fall-in output temperature, here lies, in contrast, the basic advantage of packing the bed, because providing the packing increases the

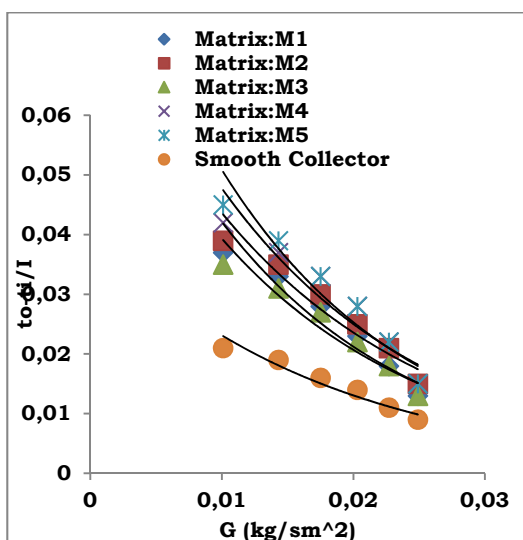


Fig.10. Variation of temperature rise parameter with mass flow rate for different matrices and smooth collector

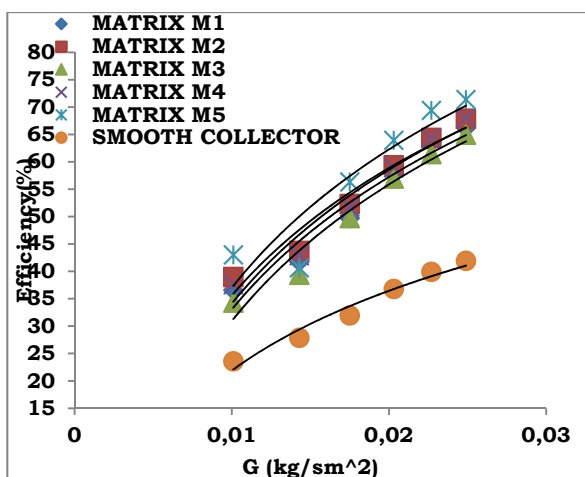


Fig.11. Variation of efficiency with mass flow rate for different matrices and smooth collector

efficiency as also increasing the output temperature a given mass flow rate at. The comparison of

enhancement given in Table 2 shows that the relative enhancement is much higher at relatively lower flow rates it is also interesting to note the efficiency plots tends the approach each other at higher flow rate indicating the similar behavior of all geometries of the matrix at very high flow rate.

### 6. Conclusions

The following are the main conclusions drawn from the present investigation:

1. It is observed that the heat transfer coefficient in packed bed solar air heater is improved appreciably as compared to conventional smooth solar collector.
2. Value heat transfer coefficient from matrix to air increases with increase in Reynolds number.
3. Friction factor is also found to increase appreciably as compared to conventional smooth collector. The value of friction factor decreases with increase in Reynolds number.
4. Thermal efficiency of solar air heater is found to improve appreciably in comparison to that of the conventional solar air heater as a result of packing the collector duct with wire screen matrixes. The improvement in thermal efficiency has been found to vary between 41.15 % and 82.40 % in the Reynolds number range of 600 to 3700.
5. Among the beds of wire screen matrixes with (wire diameter = 0.0585 mm, pitch = 3.17 mm, number of layer = 6, porosity = 0.945 ) has been found to yield maximum thermal efficiency for the range of operating parameter studied in the present work. The efficiency is seen not to depend only on porosity. The efficiency appears to depend on the geometry of the screen forming the matrix.
6. The maximum percentage enhancement for packed bed collector in comparison to the smooth solar air heater has been found to vary between 82.40 % and 71.03 % corresponding to temperature rise parameter values of 0.044 and 0.023 °C/W m<sup>2</sup>.
7. The thermal efficiency of matrix packed collector increases with increase in mass flow rate because of increased heat transfer coefficient due to increased turbulence and the lower amount of thermal losses. In the range of lower mass flow rates, the rate of increase in efficiency is higher where as in the higher range of mass flow rate the rate of increase in efficiency is lower.
8. Performance of solar air heater is function of geometrical parameters of matrix. Porosity independently does not govern the performance.

**Nomenclature**

A	heat transfer area ( $m^2$ )	$A_f$	frontal area of duct ( $m^2$ )
$A_c$	collector plate area ( $m^2$ )	$C_p$	specific heat of air ( $J.kg^{-1}.K^{-1}$ )
D	depth of bed (m)	$d_w$	wire diameter of screen (m)
$f_p$	friction factor in packed bed	g	acceleration due to gravity ( $m.s^{-2}$ )
G	air mass flow rate per unit collector area ( $kg.s.m^{-1}$ )	$G_o$	mass velocity of air ( $kg.s^{-1}.m^{-2}$ )
hc	convective heat transfer coefficient ( $W.m^{-2}.K^{-1}$ )	I	solar radiation flux ( $W.m^2$ )
J	colburn j- factor)	L	length of collector duct (m)
m	mass flow rate of air ( $kg.s^{-1}$ )	Nu	Nusselt number
P	porosity	Pr	prandtl number
$P_t$	pitch in wire mess (m)	$\Delta p$	pressure difference (kPa)
$Q_u$	useful heat gain rate per unit collector area ( $W.m^{-2}$ )	$r_h$	hydraulic radius (m)
Re	Reynolds number	$Re_p$	packed bed Reynolds number
St	Stanton number	$T_{me}$	average mess temperature (K)
$T_i, t_i$	air inlet temperature (K)	$T_f, t_f$	average fluid temperature (K)
u	velocity of air in duct ( $m.s^{-1}$ )	$\eta_s$	efficiency of smooth air heater
$\eta$	collector thermal efficiency	$\rho$	density of air ( $kg.m^{-3}$ )
$\mu$	dynamic viscosity of fluid ( $Ns.m^{-2}$ )		

**References**

- [1] ASHRAE Standard, 193-77, Method of testing to determine the thermal performance of solar collectors, 1977.
- [2] Bhatti, M.S. and Shah, R.k., Turbulent and transition convective heat transfer in ducts, Hand book of single phase convective heat transfer edited by Kakac, S., and Shah, R.K. and Aung, W., Wiley, New York, 1987
- [3] Choudhury, C., Garg, H.P. and Prakash, J., Design studies of packed –bed solar air heaters, Energy Convers. Mgmt, 34(2), 125-138, 1993.
- [4] Chiou, J. P., Wakil, M.M. and Duffie, J.A., A slit and expended aluminium foil matrix solar collector, Solar Energy 9(2), 73-80, 1965.
- [5] Coppage, J.E. and London, A.L., Heat transfer and flow friction characteristics of porous media, Chem. Engg. Progress, 52(2), 57F-63F, 1956.
- [6] Dhiman, P., Thakur, N.S. and Chauhan, S.R., Thermal and thermohydraulic performance of counter and parallel flow packed bed solar air heaters, Renewable Energy, 46, 259-268, 2012.
- [7] Reddy, T.A. and Gupta, C.L., Generating application design data for solar heating systems, Solar Energy, 25, 527-530, 1980.
- [8] Hamid, Y.H. and Beckman, W.A., Performance of air cooled radiatively heated screen matrices, Trans. ASME, J. Engineering for Power, 221-224, 1971.
- [9] Hasatani, Chiou M. Itaya, Y. and Adachi, K. Heat transfer and thermal storage characteristics of optically semi-transparent material packed-bed solar air heater, Current researches in heat and mass transfer, A Compendium and Festschrift for Prof. A. Ramachandran, ISHMT, Dept. of Mechanical Eng., IIT, Madras, India, 61-70, 1985.
- [10] Mittal, M.K. and Varshney L., Optimal thermohydraulic performance of a wire meshed packed solar air heater, Solar Energy, 80, 1112-1120, 2006.
- [11] Ozturk H.H. and Demirel, Y., Exergy-based performance analysis of packed bed solar air heater, International Journal of Energy Research, 28, 423-432, 2004.
- [12] Prasad, S.B., Saini, J.S. and Singh K.M., Investigation of heat transfer and friction characteristics of packed bed solar air heater using wire mesh as packing material, Solar Energy, 83, 773-783, 2009.
- [13] Thakur, N.S., Saini J.S. and Solanki S.C., Heat transfer and friction factor correlations for packed bed solar air heater for a low porosity system, Solar Energy, 74, 319-329, 2003.
- [14] Tong, L.S. and London, A.L., Heat transfer and flow friction characteristics of woven-screen and cross-rod matrixes, Trans. ASME, 79, 1558-1570, 1957.
- [15] Varshney, L. and Saini, J.S., Heat transfer and friction factor correlations for rectangular solar air heater duct packed with wire mesh screen matrices, Solar Energy, 62(4), 255-262, 1998.